Research article

Le Carbone prevents liver damage in non-alcoholic steatohepatitis-hepatocellular carcinoma mouse model via AMPKα-SIRT1 signaling pathway activation

Mst. Rejina Afrin [a,b,**], Somasundaram Arumugam [b,c], Vigneshwaran Pitchaimani [b], Vengadeshprabhu Karuppagounder [b,d], Rajarajan Amirthalingam Thandavarayan [b,e], Meilei Harima [b,f], Chowdhury Faiz Hossain [a], Kenji Suzuki [g], Hirohito Sone [h], Yasuhiro Matsubayashi [h], Kenichi Watanabe [b,h,*]

[a] Department of Pharmacy, Faculty of Sciences and Engineering, East West University, Dhaka 1212, Bangladesh
[b] Department of Clinical Pharmacology, Faculty of Pharmaceutical Sciences, Niigata University of Pharmacy and Applied Life Sciences, Niigata 956-8603, Japan
[c] Department of Pharmacology and Toxicology, National Institute of Pharmaceutical Education and Research, 168 Manicktala Main Road, Kolkata 700 054, West Bengal, India
[d] Department of Orthopedics and Rehabilitation, Penn State College of Medicine, 500 University Drive, Hershey, PA 17033, USA
[e] Department of Cardiovascular Sciences, Houston Methodist Research Institute, Houston, TX 77030, USA
[f] Niigata University of Rehabilitation, Faculty of Allied Health Sciences, 2-16, Kaminoyama, Murakami, Niigata 958-8292, Japan
[g] Department of Clinical Engineering and Medical Technology, Niigata University of Health and Welfare, Niigata 950-3198, Japan
[h] Department of Hematology, Endocrinology and Metabolism, Niigata University Graduate School of Medical and Dental Sciences, Niigata 951-8510, Japan

ABSTRACT

Le Carbone (LC), a fiber-enriched activated charcoal dietary supplement, claimed to be effective against inflammation associated with colitis, trimethylaminuria, and sclerosis. The study aimed to investigate the underlying mechanisms of LC to protect liver damage and its progression in non-alcoholic steatohepatitis-hepatocellular carcinoma (NASH-HCC) mice. To induce this model, C57BL/6J male baby mice were injected with a low-dose of streptozotocin and fed with a high-fat diet (HFD) 32 during 4 weeks–16 weeks of age. The LC suspension was administered orally at a dose of 5 mg/mouse/day started at the age of 6 weeks and continued until 16 weeks of age along with HFD32 feeding. At the end of the experiment, serum and liver tissues were collected for the biochemical, histological, and molecular analysis. We found that LC suspension improved the histopathological changes, serum aminotransferases in NASH mice. The hepatic expression of metabolic proteins, p-AMPKα and sirtuin 1, and proteins responsible for β-oxidation of fatty acids, peroxisome proliferator-activated receptor (PPAR) γ coactivator-α, PPARα were significantly repressed in NASH mice. LC treatment markedly restored these expressions. LC treatment significantly reduced the hepatic proteins expressions of PPARγ, tissue inhibitor of metalloproteinases 4, p47phox, p-JNK, p-ERK1/2, glypican-3, and prothrombin in NASH mice. Our findings demonstrate that LC prevents the liver damage and progression of NASH, possibly by enhancing the AMPK-SIRT1 signaling pathway.

1. Introduction

The growth of non-alcoholic fatty liver diseases (NAFLD) becomes alarming for leading sedentary and food-abundant lifestyle [1]. Non-alcoholic steatohepatitis (NASH) is an extended stage of NAFLD. Necroinflammation, lipid accumulation, and fibrosis that appear in the NASH stage may progress to cirrhosis and hepatocellular carcinoma (HCC) [2]. Although it is not still clear the transition mechanism from simple fatty liver to the NASH, it might be due to the increased levels of toxic lipids, which is occurred by the abnormal lipid metabolism where both of the oxidative stress and pro-inflammatory cytokines may act as stimulant [3, 4].

* Corresponding author.
** Corresponding author.
E-mail addresses: drja@ewubd.edu (Mst.R. Afrin), wataken@med.niigata-u.ac.jp (K. Watanabe).

The sirtuin 1 (SIRT1) and AMP-activated protein kinase (AMPK) axis play a central role in the regulation of fat catabolism in the liver [5, 6, 7]. Impairment in the SIRT1/AMPK axis has been found in several animal models with NAFLD [5]. It has been reported that the deacetylation of SIRT1 regulates several proteins that participate in NAFLD progression [8]. The level of protein expression of SIRT1 has been reported to be lowered at different NAFLD models [9]. Similarly, the AMPK signaling pathway helps to maintain metabolic homeostasis in cellular and organismal levels at the time of stress [10].

It has been found that activation of the SIRT1-AMPK signaling pathway enhances the β-oxidation of fatty acid in hepatocytes and other metabolic tissues. Thus restrain lipid synthesis mostly via controlling the activity of peroxisome proliferator-activated receptor gamma coactivator-α (PGC-1α)/peroxisome proliferator-activated receptor alpha (PPARα) or sterol regulatory element binding protein-1 (SREBP-1) through deacetylation and phosphorylation, respectively [11, 12].

PPARγ, a ligand-activated transcription factor, acts as a master regulator of fat storage and energy homeostasis [13]. Increased expression of PPARγ is found in obese mice and associated with an increase of lipogenesis. PPARα regulates β-oxidation and removes cholesterol at the time of necessity. It is also noticed that the protein expression of PPARα in the liver with NAFLD is lower due to lipogenesis, which can be recovered by following a proper diet and regular exercise [14].

It was reported that vitamin E enriched dietary supplement improved the NAFLD activity score in non-diabetic patients with biopsy-proven NASH [15]. Le Carbone (LC), a commercial fiber-enriched activated charcoal dietary supplement, was found to enhance the AMPK-SIRT1 expression in colon tissue of experimental colitis in a mouse model, and to reduce the inflammation [16]. Activated charcoal also reported to has wound healing and anti-aging properties [17]. It has been proved that activated charcoal along with mitomycin-C reduced the development of secondary cancer after stomach surgery, where only the anti-cancer drug failed to do it [18]. Furthermore, in patients with trimethylaminuria (a metabolic disorder), activated charcoal supplements improved the health condition of them [19]. Activated charcoal also used to protect atherosclerosis by improving the lipid profile [20]. Due to having the beneficial effects of the LC supplement, we assume that LC might be able to protect liver damage in an experimental NASH-HCC mouse by activating AMPK-SIRT1 expression.

2. Materials and methods

2.1. Drugs and chemicals

High-fat diet (HFD) 32 was purchased from CLEA, Japan. LC was provided by Bloom Biotechnology Ltd, Japan. All other chemicals used were purchased from Sigma, Japan unless mentioned otherwise.

2.2. Composition of normal diet, HFD32 and LC

The normal diet was contained (water 10.0%, protein 25.0%, fat 4.5%, ash 6.7%, carbohydrate 49.3% and fiber 4.5%), and provided 404 Kcal/100 g at the same time the HFD 32 was contained (water 6.2%, protein 25.5%, fat 32.0%, ash 4.0%, carbohydrate 29.4%, and fiber 2.9%) and provided 507.6 Kcal/100 g. The LC was in capsule form; composed of activated Carbone and a minor quantity of minerals. Among the 100 g of LC, 2.2 mg of sodium, 77.6 mg of potassium, and 0.4 mg of manganese and other minerals such as non-phosphorous, iron, calcium, magnesium, copper, zinc, and heavy metals (cadmium, lead, arsenic, and total mercury) were absent. The nutritional content of LC was tested by the Corporation Vision Bio-test where energy 4 Kcal, moisture 0.6 g, protein minimum, lipid minimum, carbohydrate 1.1 g, ash 0.2 g, water-soluble dietary fiber 0.6 g, insoluble dietary fiber 97.5 g and the dietary fiber total amount 98.1 g were found in 100 g of LC.

2.3. Animals and experimental protocol

All mice were handled followed by the guidelines for animal experimentation of Niigata University of Pharmacy and Applied Life Sciences (Approve No. H270313) [21]. Mice were placed in the animal house maintained at $23 \pm 2\,°C$, with a 12h light/dark cycle and humidity $55 \pm 15\%$. They were provided with standard laboratory chow and tap water ad libitum. C57BL/6J mice were bred in our laboratory. For the induction of NASH-HCC, at 2 days after birth, the male mice were injected with a single subcutaneous dose of 200 μg streptozotocin (STZ) (Sigma, MO, USA). After 4 weeks of injection, they were being started feeding with HFD32 ad libitum, and continued up to 16 weeks age of mice. Mice were divided into three groups and each group contained 6 mice, the first one, (Normal group), where normal (STZ non-injected) mice were fed with normal diet; the second one (NASH group), where STZ injected mice were fed with HFD32, treated with 1% methyl cellulose (MC) (the vehicle of LC); the third one (NASH + LC group), where STZ injected mice were fed with HFD32 and administered with LC suspension at (5 mg/mouse/day, suspended in 1% MC). The LC treatment was provided from the age of 6 weeks–16 weeks via oral gavage (Figure 1). At the age of 16 weeks, the mice of all groups were sacrificed and then the serum and liver tissues were collected for further analysis [22].

2.4. Estimation of biochemical parameters

The blood glucose level in the fasting condition was measured using the G-checker (Sanko Junyaku, Tokyo, Japan). The serum alanine aminotransferase (ALT), aspartate aminotransferase (AST), alkaline phosphatase (ALP), triglyceride (TG) and total cholesterol (TC) were measured by FUJI DRI-CHEM 7000 (Fujifilm, Tokyo, Japan) as previously described [21].

2.5. Histological examination

Formalin-fixed 4 μm liver tissue sections were stained with hematoxylin and eosin (H&E). Histological analysis was done by the observer who is blind to the study group using a computerized image analysis system on ten microscopic fields per section examined in a 20-fold magnification (CIA-102; Olympus, Tokyo, Japan) [21]. The scoring of NAFLD was done using a method similar to that described previously [23]. The NASH was confirmed when the NAFLD activity score is equal to or more than 5.

2.6. Determination of liver fibrosis content

To detect fibrosis the formalin-fixed, paraffin-embedded, liver tissue sections (4 μm) were stained with Masson trichrome (MT) [24]. MT staining was done according to the manufacturer's instructions (Accustain HT15, Sigma-Aldrich, St. Louis, MO).

2.7. Western blot analysis

The liver tissue protein lysate was prepared using a method like that described previously [25]. The total protein concentration in the liver homogenate was estimated by the bicinchoninic acid (BCA) method. The equal amounts of protein lysate of the liver (50 μg) were separated by sodium dodecyl sulfate (SDS) polyacrylamide (7.5–15%) gel electrophoresis (Bio-Rad, CA, USA) and transferred to nitrocellulose membranes to determine the protein levels. 5% bovine serum albumin (BSA) or skim-milk in Tris-buffered saline Tween (20 mM Tris, pH 7.6, 137 mM NaCl, and 0.1% Tween 20) were used to block the membranes. The source of primary antibodies such as SIRT1, Heme-oxygenase-1 (HO-1), p47phox, nuclear factor-erythroid 2-related factor (Nrf)-2, glucose transporter type (GLUT) 4, phosphoenol pyruvate carboxykinase (PEPCK)-C, PPARα, PPARγ, adipose differentiation-related protein (ADRP), tissue inhibitor of metalloproteinases (TIMP) 4, and glypican-3
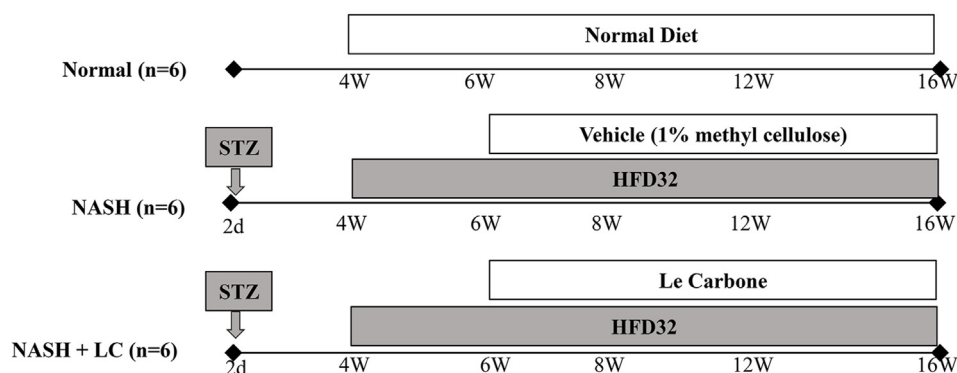
Figure 1. Experimental protocol. Experimental protocol used in the present study. Streptozotocin (STZ) was injected *s. c.* to the 2 days old pups and then allowed to grow under breast milk. At 4 weeks of age the mice were given either normal diet or high-fat diet (HFD) 32. Le Carbone suspension (LC) treatment was given to the NASH + LC group mice from 6 weeks of age to 16 weeks of age. All the mice were sacrificed at 16 weeks of age.

was from Santa Cruz Biotechnology, Santa Cruz, CA, USA. And the phospho-AMPKα, AMPKα, PGC1α, c-Jun-N-terminal kinases (JNK), p-JNK, extracellular signal-regulated kinase (ERK) 1/2, p-ERK1/2, β-actin and glyceraldehyde-3-phosphate dehydrogenase (GAPDH) antibodies were purchased from Cell Signaling Technology Inc., Beverly, MA, USA. Prothrombin was obtained from Abcam, Cambridge, UK. The equal loading of the sample was confirmed in every membrane by using AMPKα (for p-AMPKα), JNK (for p-JNK), ERK1/2 (for p-ERK1/2), and GAPDH or β-actin.

2.8. Immunohistochemistry

To do immune histochemical analysis formalin-fixed, paraffin-embedded liver tissue sections were used to stain. For this purpose, the hepatic tissue sections were at first deparaffinized and then hydrated. To wash the slides Tris-buffered saline (TBS; 10 mM/L Tris-HCl, 0.85% NaCl, pH 7.2) was used. To quench the endogenous peroxidase activity the slides were incubated in methanol and 0.3% H_2O_2 in methanol. The slides were incubated with the primary antibody, mouse monoclonal anti-cluster of differentiation (CD)36 (diluted 1:100) (sc-59103; Santa Cruz Biotechnology Inc. CA, USA) at 4 °C overnight, then the slides were washed with TBS and the slides were further incubated at room temperature for 1 h after adding the horseradish peroxidase (HRP) -conjugated goat anti-rabbit secondary antibody. Then the slides were again washed with TBS and incubated with a substrate called diaminobenzidine tetra hydrochloride, after that hematoxylin was used to counterstain the slides. To verify the antibody specificity a negative control (lack of primary antibody) was included in the experiment. From every group, 100 fields were analyzed to count the CD36 positive

hepatocytes under 20-fold magnification, which are expressed as cells/field [16].

2.9. Statistical analyses

Data were expressed as means ± standard error of the mean (SEM) and were analyzed using one-way analysis of variance (ANOVA) followed by Tukey's method. A value of $p < 0.05$ was considered statistically significant, GraphPad Prism 5 software (San Diego, CA, USA) was used.

3. Results

3.1. Effect of LC on histopathology and biochemical parameters in NASH-HCC mice

No significant difference was found for energy consumption and body weight among the experimental groups during this experimental period (Table 1). Macroscopically, the liver of the mice in the NASH group found with abnormal shape and swelling, with tumor protrusion; on the other hand, the liver of the LC group was moderately fatty, and no tumor was found there (Figure 2A). The ratio of liver index (g/Kg) was markedly higher in NASH group when compared to the mice of normal group ($p < 0.01$), but in the mice of LC treated group this elevated ratio were significantly lesser ($p < 0.05$ vs. NASH) (Table 1, Figure 2B). The significant elevation of fasting blood glucose level and TG, TC, ALT, and ALP levels in serum were also showed in the mice of the NASH group in comparison to normal group (Table 1). The serum ALT and AST levels, indicators of liver damage, were significantly prevented in LC treated group ($p < 0.05$), and other lipid profile markers were also noticeably

Table 1. Changes in biochemical parameters after treatment with Le Carbone in NASH-HCC mice.

	Normal group (n = 6)	NASH group (n = 6)	NASH + LC group (n = 6)
Food intake/day/mouse (g)	3.133 ± 0.151	2.575 ± 0.053	2.505 ± 0.154
EC/day/mouse (Kcal)	12.66 ± 0.611	13.1 ± 0.27	12.72 ± 0.783
Body weight (BW) (g)	24.23 ± 0.75	22.70 ± 4.66	22.33 ± 1.62
Liver index (LW)/BW (g/Kg)	53.48 ± 2.61	86.85 ± 14.32**	63.33 ± 11.29#
Blood glucose (mg/dL)	110.75 ± 13.67	469.60 ± 65.00***	490.50 ± 14.18***
Serum TG (mg/dL)	47.33 ± 13.8	59.00 ± 18.33	30.50 ± 13.53
Serum TC (mg/dL)	90.00 ± 7.81	202.00 ± 29.02***	148.50 ± 19.94#*
Serum ALT (IU/L)	62.00 ± 3.46	367.00 ± 173.53*	65.75 ± 27.29#
Serum AST (IU/L)	145.67 ± 46.29	799.25 ± 353.26*	186.00 ± 66.39#
Serum ALP (IU/L)	358.33 ± 35.84	646.25 ± 215.13	334.25 ± 89.20#

Normal, age matched normal mice; NASH, untreated NASH-HCC mice; NASH + LC, NASH-HCC mice treated with Le Carbone suspension at 5 mg/mouse/day. TG: triglyceride; TC: total cholesterol, ALT: alanine aminotransferase, ALP: alkaline phosphatase, AST: aspartate aminotransferase, EC: Energy consumption. Values are expressed as means ± SEM\. *$p < 0.05$, **$p < 0.01$, ***$p < 0.001$ vs normal, #$p < 0.05$ vs NASH.
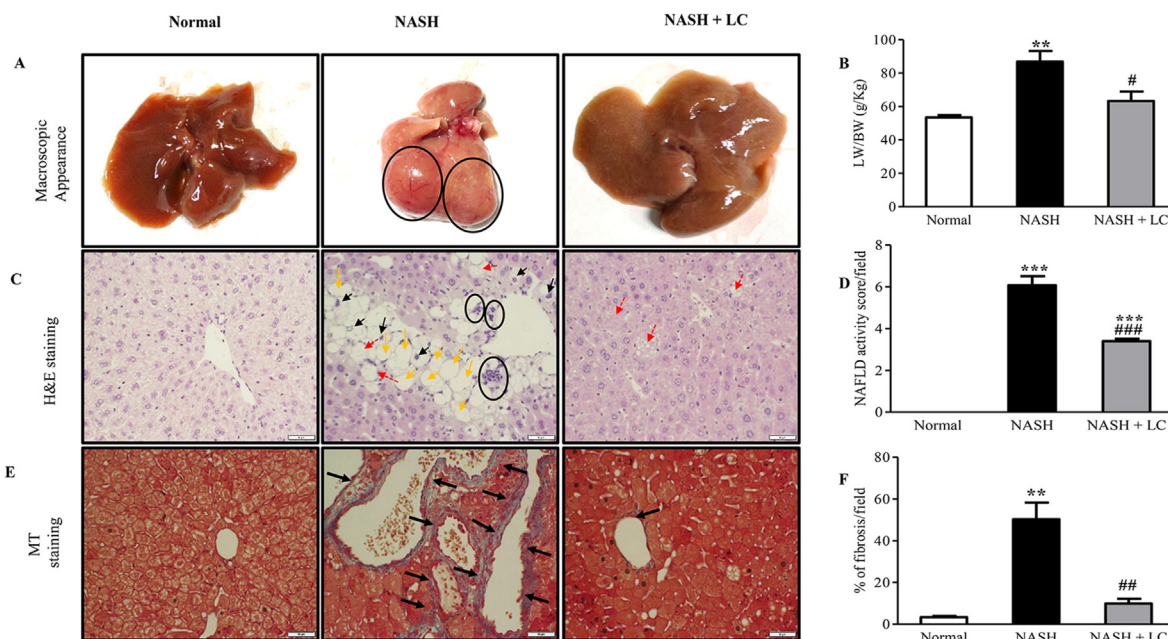
Figure 2. Le Carbone attenuates the clinicopathology in NASH-HCC mice. (A), Representative macroscopic appearance of livers (circles: liver tumors). (B), Histogram for the ratio of liver weight (LW) and body weight (BW) in g/Kg. (C), H&E staining (yellow arrow: macro vesicular steatosis, black arrow: micro vesicular steatosis, red arrow: hypertrophy, circles: inflammatory cells). Scale bars, 50 μm. (D), Histogram of non-alcoholic fatty liver disease (NAFLD) activity score. (E), Fibrosis deposition by Masson trichrome staining (blue area, black arrow). Scale bars, 50 μm. (F), percentage of fibrosis in each group. Data are mean ± SEM, (n = 6/group). Normal, age matched normal mice; NASH, untreated NASH-HCC mice; NASH + LC, NASH-HCC mice treated with Le Carbone suspension at 5 mg/mouse/day. Statistical analysis was carried out using One-way ANOVA followed by Tukey's test where $**p < 0.01$, $***p < 0.001 vs$ Normal, and $\#p < 0.05$, $\#\#p < 0.01$, $\#\#\#p < 0.001 vs$ NASH.

lesser in the LC group than the NASH group (Table 1). But the administration of LC did not show any effect on the increased blood glucose level (Table 1). From the H&E stained slides of hepatic tissues, extreme steatosis, cellular hypertrophy, and scattered lobular, inflammatory cells were found in the mice of the NASH group, which indicate the NAFLD activity score. Whereas all these changes and the NAFLD activity score were significantly lesser in the mice of the NASH + LC group in comparison to the NASH group (Fig. 2C-D).

3.2. Effect of LC on hepatic fibrosis in NASH-HCC mice

From the MT staining of hepatic tissues, we determined the hepatic fibrosis among the three groups. MT staining showed pericellular fibrosis
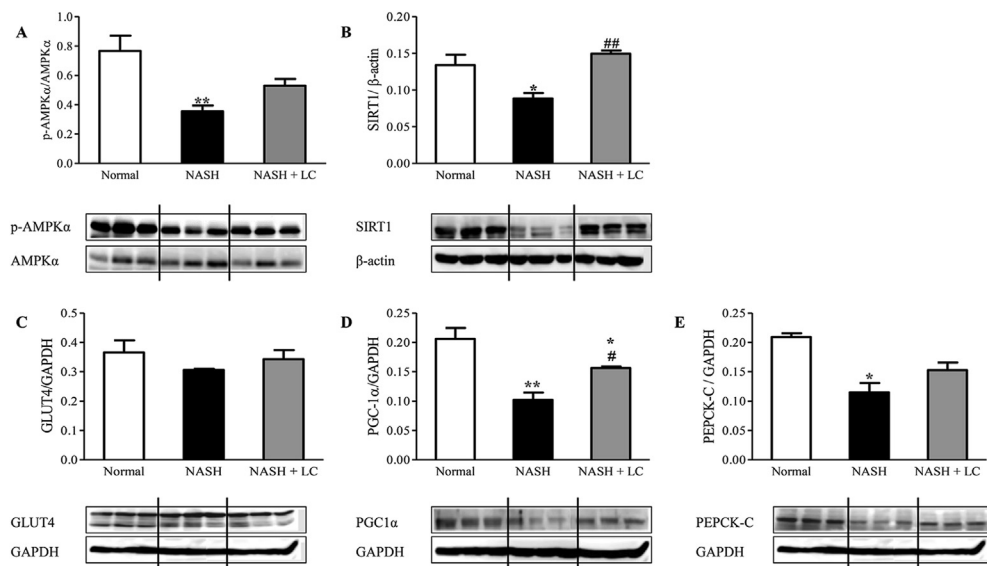
around central veins. The percentage of fibrosis in the blue-stained (positive) area was significantly increased in the NASH group in comparison to the normal group ($p < 0.01$). In contrast, this percentage was significantly lesser in the NASH + LC group ($p < 0.01$ vs. NASH) (Fig. 2E-F).

3.3. LC administration stimulated hepatic p-AMPKα and SIRT1 expression in NASH-HCC mice

Since AMPK and SIRT1 play a vital role in the lipid metabolism in the hepatocyte, we investigated the protein expression levels in NASH livers using Western blot. The protein expression of p-AMPKα ($p < 0.01$) and SIRT1 ($p < 0.05$) were significantly lesser in the NASH group when

Figure 3. Effect of Le Carbone on hepatic AMPKα, SIRT1, GLUT4, PGC1α and PEPCK-C expression in NASH-HCC mice. Representative Western blots show specific bands for hepatic (A), p-AMPKα (for AMPKα); (B), SIRT1 (for β-actin); (C), GLUT4; (D), PGC1α; and (E), PEPCK-C and the representative histograms show the band densities with relative to GAPDH. Each bar represents mean ± SEM. Normal, age matched normal mice; NASH, untreated NASH-HCC mice; NASH + LC, NASH-HCC mice treated with Le Carbone suspension at 5 mg/mouse/day. Statistical analysis was carried out using One-way ANOVA followed by Tukey's test where, $*p < 0.05$, $**p < 0.01$ vs Normal, and $\#p < 0.05$, $\#\#p < 0.01$ vs NASH.

compared to that of the normal group. The hepatic protein expression of p-AMPKα was higher in the LC treated group by 1.5-fold when compared to the NASH group but did not reach a significant level (Figure 3A). The hepatic protein levels of SIRT1 were markedly increased in the mice of the NASH + LC group when compared to the NASH group ($p < 0.01$) (Figure 3B).

3.4. Effect of LC on hepatic GLUT4, PGC1α, and PEPCK-C expression in NASH-HCC mice

The upregulation of AMPK and SIRT1, reduce the hepatic lipid accumulation [5, 26]. To check this effect, we detected the downstream proteins of AMPK using Western blot, including GLUT4, PGC1α, and PEPCK-C, which are all associated with lipid metabolism. The protein expression of GLUT4 was trended to lesser in the liver of the NASH group by 0.84-fold, while PGC1α ($p < 0.01$) and PEPCK-C ($p < 0.05$) expression were significantly lesser when compared to the normal mice. But, in the NASH + LC group, hepatic protein expression of GLUT4 was trended to increase by 1.1-fold compared to NASH mice (Figure 3C). The protein levels of PGC1α ($p < 0.05$) and PEPCK-C were about 1.4-fold higher in LC treated liver than the liver of NASH group (Fig. 3D-E).

3.5. Effect of LC on hepatic expression of PPARα, PPARγ, ADRP and TIMP4 protein levels in NASH-HCC mice

We examined the effect of LC on the central regulator of lipid metabolism, PPARα, and steatosis-related protein expression such as PPARγ and ADRP in the liver of NASH mice. We observed that the hepatic expression of PPARα ($p < 0.05$) was significantly lesser in NASH mice than the normal mice, whereas, in the mouse of the LC treated group, the reduced PPARα level was significantly increased than the NASH mice ($p < 0.01$). Interestingly, we found that the hepatic expression of PPARα in the NASH + LC group was also significantly higher than the normal mice ($p < 0.05$) (Figure 4A). The expression of PPARγ ($p < 0.05$), ADRP ($p < 0.01$), and TIMP4 ($p < 0.05$) proteins were increased in the NASH liver than the normal mice. In LC treated mice, the increased levels of PPARγ

and TIMP4 were significantly prevented ($p < 0.01$, $p < 0.05$), and the level of ADRP was 0.77-fold lesser but did not reach in a significant level when compared to the NASH mice (Fig. 4B-D).

3.6. Effect of LC on the expression of CD36 positive cells in NASH-HCC liver

The immunohistochemistry data showed that the CD36 positive cells were significantly lower in the hepatic tissue of NASH group than the normal group ($p < 0.01$), but in LC treated group CD36 positive cells were markedly higher than in the NASH hepatic tissue ($p < 0.05$) (Figure 5A-B).

3.7. Effect of LC on hepatic oxidative and anti-oxidative marker expression in NASH-HCC mice

Since oxidative stress plays an important role in the progression of NASH, and activation of the AMPK-SIRT1 signaling pathway reduced intracellular reactive oxygen species (ROS) levels [27], we checked some protein expression levels by Western blot in all groups. These included anti-oxidative marker proteins HO-1, Nrf2, and NAD(P)H oxidative subunit p47phox. The hepatic protein expression of HO-1 ($p < 0.05$) and Nrf2 ($p < 0.05$) were significantly lower, and p47phox was higher ($p < 0.01$) in NASH mice when compared to normal mice. But the protein expression level of HO-1 ($p < 0.05$) and Nrf2 ($p < 0.01$) were significantly higher in the NASH + LC group than the NASH group (Figure 6 A& C). Interestingly, the increased p47phox level was also markedly lesser in the NASH + LC group ($p < 0.01$) in comparison to the liver of NASH group (Figure 6B).

3.8. Effect of LC on the protein expression levels of p-JNK and p-ERK1/2 in NASH-HCC liver

The hepatic protein expression of p-JNK and p-ERK1/2 was significantly elevated in the mice of the NASH group ($p < 0.01$, $p < 0.05$), respectively than the normal group. While in LC treated group, both
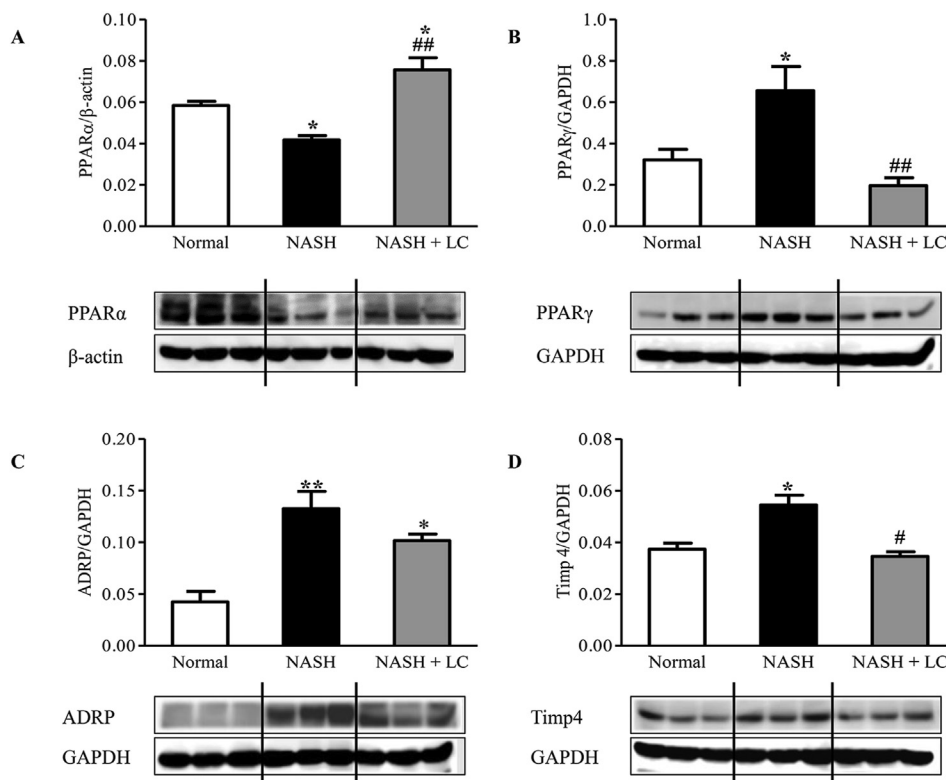

Figure 4. Le Carbone attenuates hepatic lipogenesis in NASH-HCC mice. Western blots show specific bands for hepatic (A), PPARα (for β-actin); (B), PPARγ; (C), ADRP; and (D), TIMP4 and the representative histograms show the band densities with relative to GAPDH. Each bar represents mean ± SEM. Normal, age matched normal mice; NASH, untreated NASH-HCC mice; NASH + LC, NASH-HCC mice treated with Le Carbone suspension at 5 mg/mouse/day. Statistical analysis was carried out using One-way ANOVA followed by Tukey's test where, *$p < 0.05$, **$p < 0.01$vs Normal, #$p < 0.05$, ##$p < 0.01$vs NASH.
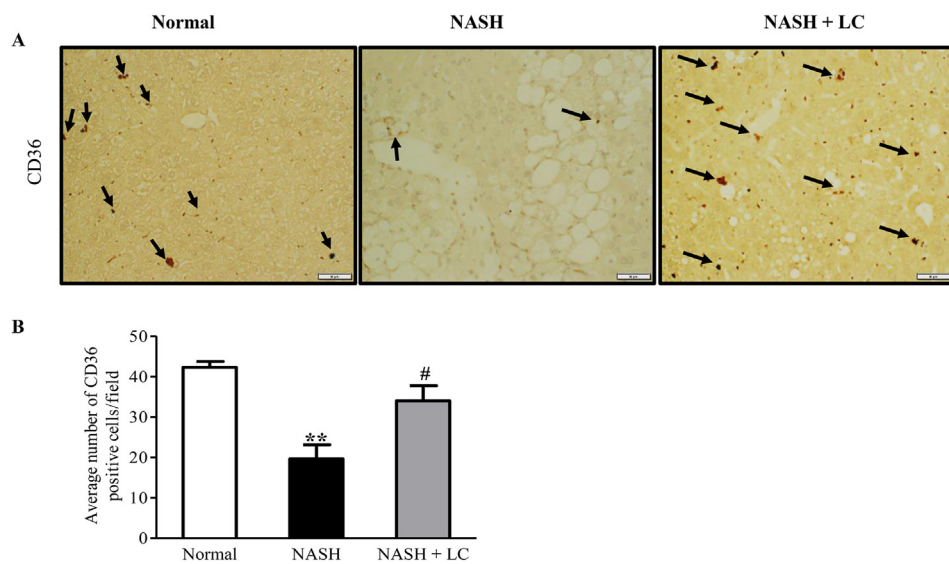
Figure 5. Effect of LC on the expression of CD36 positive cells in NASH-HCC liver. (A–B), Immunohistochemical staining of CD36 positive cells and their quantitative data. Data are mean ± SEM, (n = 6/group). Normal, age matched normal mice; NASH, untreated NASH-HCC mice; NASH + LC, NASH-HCC mice treated with Le Carbone suspension at 5 mg/mouse/day. Scale bars, 50 μm. Statistical analysis was carried out using One-way ANOVA followed by Tukey's test where, **$p < 0.01$ vs Normal, #$p < 0.05$ vs NASH.
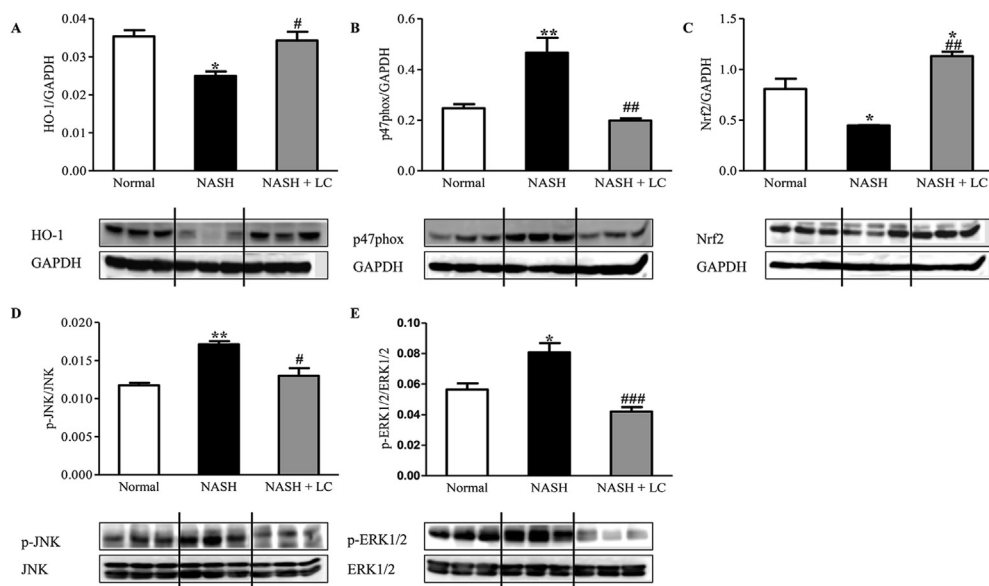

Figure 6. Effect of Le Carbone on hepatic HO-1, p47phox, Nrf2, p-JNK and p-ERK1/2 expression in NASH-HCC mice. Representative Western blots show specific bands for (A), HO-1; (B), p47phox; (C), Nrf2; (D), p-JNK (for JNK); (E), p-ERK1/2 (ERK1/2) and the representative histograms show the band densities with relative to GAPDH. Each bar represents mean ± SEM. Normal, age matched normal mice; NASH, untreated NASH-HCC mice; NASH + LC, NASH-HCC mice treated with Le Carbone suspension at 5 mg/mouse/day. Statistical analysis was carried out using One-way ANOVA followed by Tukey's test where, *$p < 0.05$, **$p < 0.01$ vs Normal, #$p < 0.05$, ##$p < 0.01$ and ###$p < 0.001$ vs NASH.
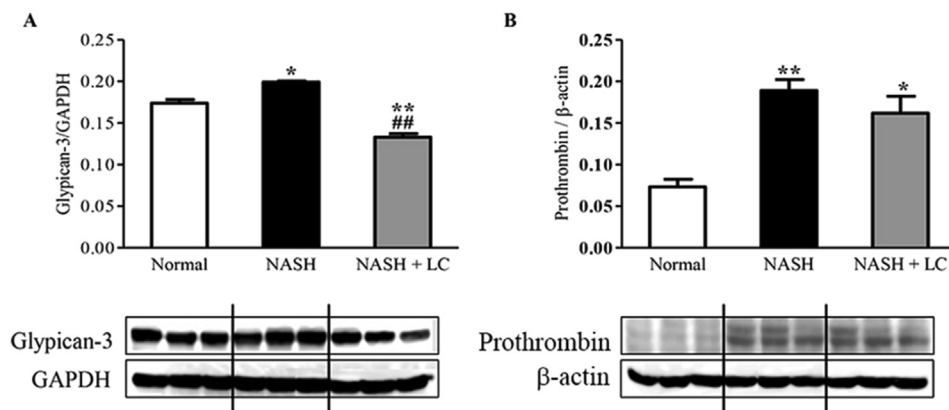

Figure 7. Effect of LC on glypican-3 and prothrombin in NASH-HCC liver. Western blots show specific bands for hepatic (A), Glypican-3; and (B), prothrombin (for β-actin), and the representative histograms show the band densities with relative to GAPDH. Each bar represents mean ± SEM. Normal, age matched normal mice; NASH, untreated NASH-HCC mice; NASH + LC, NASH-HCC mice treated with Le Carbone suspension at 5 mg/mouse/day. Statistical analysis was carried out using One-way ANOVA followed by Tukey's test where, *$p < 0.05$, **$p < 0.01$ vs Normal, ##$p < 0.01$ vs NASH.

protein levels were markedly reduced than that of the NASH group (p < 0.05, p < 0.001) (Fig. 6D-E).

3.9. Effect of LC on glypican-3 and prothrombin in NASH-HCC liver

The expression of both hepatic proteins, glypican-3 ($p < 0.05$) and prothrombin ($p < 0.01$), were significantly elevated in the NASH group (Figure 7A-B) in comparison to that of the normal group. Whereas, the expression of both hepatic proteins, glypican-3 and prothrombin, were prevented in the LC treated group in comparison to that of the NASH group (Figure 7A-B).

4. Discussion

To understand the pathogenesis and the effect of a treatment, mouse models for NASH-HCC play an important role. There is a large phenotypical assortment in the accessible mouse models, anyway, models that show the full range of histopathological and metabolic features related to human NASH are rare. As NASH is considered as a hepatic sign of the metabolic issue and exceedingly associated with diabetes, it is likewise presumed that there is a relationship among diabetes and HCC with the development of NASH [28]. Some reports suggested that charcoal has the ability to detoxify the fatty liver in obese and alcoholic subjects and can also capable of reducing the levels of total lipids, cholesterol, and triglycerides both in serum and tissues like liver, heart and brain [20, 29]. In our previous experiment, it was found that LC reduced DSS-induced colitis in mice with an oral dose of 5mg/mouse/day, this dose was resembled with a dose of 8 g thrice a day (24 g) in patients with hypercholesterolemia [16, 20]. In this experiment, we researched the effective mechanism of LC against the hepatoprotection in the NASH-HCC mouse model using the same dose. This is the first study to report the role of LC against the progression of NASH to HCC.

AMPK is the master regulator of energy homeostasis, plays a concerning role in diabetes, metabolic syndrome, cardiovascular diseases, and cancers [30, 31]. Reduced AMPK activity leads to lipid synthesis, which may promote the steatosis and possible lipotoxicity; therefore, hepatocellular injury and prolongation of liver inflammation may appear, in the NASH-HCC mouse model. AMPK and SIRT1 are evolutionarily conserved partners, and both play an important role in metabolism and cellular survival [6]. And energy metabolism has a basic role in malignancy advancement, AMPK/SIRT1 may be a promising focus for HCC treatment. In a clinical study, it is also found that the protein concentration of phosphorylated AMPK is lesser in hepatocyte of HCC than the normal [32]. The protein expression of p-AMPK and SIRT1 were significantly lower in NASH liver than the normal liver. LC treatment enhanced the p-AMPK and SIRT1 expressions in the NASH + LC group (Fig. 3A-B). Activation of the AMPK pathway prevents oxidative stress-induced cellular damage by reducing intracellular ROS; triggered by different insult; hyperglycemia, fatty acids [27, 33]. ROS also downregulates SIRT1 protein expressions [34]. There are several target proteins of AMPK like SIRT1, PGC1α, HO-1, and FOXOs, called longevity factors, that are responsible for increasing the resistance against stress, as well as inhibit inflammatory response [35]. The nutrient sensor, SIRT1, also exerts the critical control in gene expression of gluconeogenesis through deacetylation of PGC-1α [36]. It is reported that the activation of PGC-1α in hepatic tissue reduced the triglyceride synthesis and release [37]. And in another study, it is also shown that in the hepatocyte of PGC-1α deficient mice, the β-oxidation of fatty acid is reduced [38]. Accordingly, we also noticed that the hepatic protein level of PGC-1α was markedly reduced in the mice of the NASH group, whereas, at LC treated group this expression was markedly elevated (Figure 3D). In addition, the expression of GLUT4 and PEPCK-C were trended to reduce in the NASH group, but tended to restore in LC treated group, and play a role in glucose utilization (Fig. 3C&E).

Moreover, suppression of AMPK levels reduces oxidation of the free fatty acid in mitochondria of hepatocytes due to increasing lipid

accumulation. It increases the ROS production that may lead to the progression of NAFLD to NASH [39]. Here, we found the LC treatment markedly enhanced the expression of PPARα in the liver of the NASH group, which is a powerful fatty acid oxidation inducer involved in lipid breakdown (Figure 4A). Activation of PPARγ is found in both alcoholic and non-alcoholic fatty liver, which is related to fat accumulation [40, 41]. There are some reports that heterozygous PPARγ-deficient mice are protected from HFD, aging-induced adipocyte hypertrophy, obesity, and insulin resistance [42, 43]. Deletion of TIMP4 improves the obesity in HFD-induced experimental mice through impairment of lipid absorption [44]. Interestingly, our present study showed that the hepatic protein expression of PPARγ, ADRP, and TIMP4, were markedly elevated in the NASH mice group, but significantly reduced in the livers of LC treated mice (Fig. 4B-D). These data might suggest that LC protects the liver from steatosis other than non-adiponectin–mediated mechanisms. These findings were related to the improvement of liver histopathology through reduced macro-and micro-steatosis, and serum ALT, AST levels in LC treated group (Figure 2C, Table 1).

Inflammation seems to play a leading role in NASH progression; therefore, the accumulation of inflammatory macrophages occurs to create inflammatory foci and to phagocyte lipid droplets [45]. At a later phase, reduced phagocytosis of macrophage was seen in human NASH [46], which indicates the altered function of macrophages. Macrophages residing by activated fibroblasts and both participate in fibrotic foci in the liver. On macrophages CD36 involves in phagocytosis. Studies showed that deletion of CD36 in mice increased MCP-1 in hepatocytes, promotes macrophage migration to the liver, and aggravates hepatic inflammatory response and fibrosis [47]. In our study, we observed that liver inflammation and fibrosis were substantially increased in the NASH group. Here, we found that the administration of LC in NASH-HCC mice displayed attenuation of inflammation and fibrosis in the liver by H&E and MT staining (Fig. 2C-F), and elevation of CD36 positive cells in the hepatic tissue (Fig. 5A&B).

Several studies have proved the contribution of oxidative stress and pro-inflammatory cytokines to the advancement of steatosis to steatohepatitis. In our study, we found the expression of NAD(P)H oxidase subunit p47phox was significantly lesser in LC treated mice (Figure 6B). Activation of antioxidants and phase II detoxifying enzymes provide protection against ROS induced tissue damage. Nrf2 is a cytoprotective transcriptional factor, increases the expression of several antioxidants and phase II detoxifying enzymes and plays a defense role in the development of NASH [48, 49]. Besides directing the cellular antioxidant guard, Nrf2s has anti-inflammatory capacities too [48]. Moreover, HO-1 acts as an antioxidant marker and can also inhibit the inflammatory response; some studies reported that the expression of HO-1 is upregulated in NASH [50]. In contrast, it is reported that the over-expression of HO-1 suppresses HCC progression by inhibiting the proliferation and metastasis of HepG2 [51]. In our experiment, it is found that hepatic protein expression of HO-1, and Nrf2 were significantly higher in the LC treated mice than the NASH-HCC mice (Fig. 6A, C). Oxidative stress and phosphorylation of JNK and ERK1/2 become evident and enhance inflammatory cytokine accumulation [52]. It is reported that the JNK and ERK also act as oncogenic mediators in HCC [53]. Phosphorylation of JNK and ERK were enhanced by HFD feeding in HCC progenitor cells derived tumors [53]. Consistent with these reports, in our study, we found the tumors protrusion in NASH liver (Figure 2A) and the hepatic expression of p-JNK, and p-ERK1/2 were also elevated in the mice of NASH group (Fig. 6D-E). But the expressions of these increased protein levels were markedly lower, and no tumor protrusion was found in LC treated group (Fig. 6D-E, 2A).

Oxidative stress and inflammatory pathways may be responsible for the transformation of a normal cell to a tumor cell and is associated with its survival and proliferation. This tumor protruding may be malignant or progress to HCC as it is shown that the hepatic expression of glypican-3 and des-γ-carboxy prothrombin or prothrombin are significantly elevated in most HCCs compared to benign liver lesions and normal livers. Thus,

these will serve as a useful prognostic tumor marker for HCC [54, 55]. In this experiment, we noticed that the expression of glypican-3 and prothrombin were higher in the NASH group compared to the normal group (Fig. 7A-B). All these protein expressions were altered in the mice of the LC treated group when compared to the NASH group.

5. Conclusion

In conclusion, our present study demonstrates the preventive action of LC suspension against NASH-HCC mice, at least in part, by stimulating the AMPK-SIRT1 signaling axis and consequently by reducing the lipogenesis, oxidative stress and inflammation in NASH liver. Thus, by repressing the movement of NASH to HCC, LC may be a valuable option in the management of NASH and may comprise a significant treatment methodology for the novel NASH-HCC model.

5.1. Limitation of work

We used LC 5mg/mouse/day one dose only. We could not check dose-dependent manner. Usually, mice were divided into three groups, Normal, NASH, and NASH + LC. We could not include another group, Normal + LC to investigate the toxicological effect of LC. In another experiment, these limitations will be overcome.

Declarations

Author contribution statement

M.R. Afrin: Conceived and designed the experiments; Performed the experiments; Analyzed and interpreted the data; Contributed reagents, materials, analysis tools or data; Wrote the paper.

S. Arumugam, V. Pitchaimani, V. Karuppagounder, R.A. Thandavarayan, C.F. Hossain: Analyzed and interpreted the data; Wrote the paper.

M. Harima: Analyzed and interpreted the data; Contributed reagents, materials, analysis tools or data.

K. Suzuki, H. Sone, Y. Matsubayashi: Contributed reagents, materials, analysis tools or data; Wrote the paper.

K. Watanabe: Conceived and designed the experiments; Contributed reagents, materials, analysis tools or data; Wrote the paper.

Data availability statement

Data included in article/supplementary material/referenced in article.

Declaration of interests statement

The authors declare no conflict of interest.

Additional information

No additional information is available for this paper.

References

[1] G.C. Farrell, V.W.S. Wong, S. Chitturi, NAFLD in Asia -As common and important as in the West, Nat. Rev. Gastroenterol. Hepatol. 10 (2013) 307–318.

[2] G.C. Farrell, C.Z. Larter, Nonalcoholic fatty liver disease: from steatosis to cirrhosis, Hepatology 43 (2006) S99–S112.

[3] G.C. Farrell, D. van Rooyen, L. Gan, S. Chitturi, NASH is an inflammatory disorder: pathogenic, prognostic and therapeutic implications, Gut Liver 6 (2) (2012) 149–171.

[4] A.P. Rolo, J.S. Teodoro, C.M. Palmeira, Role of oxidative stress in the pathogenesis of nonalcoholic steatohepatitis, Free Radic. Biol. Med. 52 (2012) 59–69.

[5] X. Hou, S. Xu, K.A. Maitland-Toolan, K. Sato, B. Jiang, Y. Ido, F. Lan, K. Walsh, M. Wierzbicki, T.J. Verbeuren, R.A. Cohen, M. Zang, SIRT1 regulates hepatocyte lipid metabolism through activating AMP-activated protein kinase, J. Biol. Chem. 283 (29) (2008) 20015–20026.

[6] N.B. Ruderman, X.J. Xu, L. Nelson, J.M. Cacicedo, A.K. Saha, F. Lan, Y. Ido, AMPK and SIRT1: a long-standing partnership? Am. J. Physiol. Endocrinol. Metab. 298 (2010) E751–E760.

[7] X. Li, SIRT1 and energy metabolism,, Acta Biochim. Biophys. Sin. 45 (1) (2013) 51–60.

[8] M.A. Suter, A. Chen, M.S. Burdine, M. Choudhury, R.A. Harris, R.H. Lane, J.E. Friedman, K.L. Grove, A.J. Tackett, K.M. Aagaard, A maternal high-fat diet modulates fetal SIRT1 histone and protein deacetylase activity in nonhuman primates, Faseb. J. 26 (2012) 5106–5114.

[9] Y. Colak, O. Ozturk, E. Senates, I. Tuncer, E. Yorulmaz, G. Adali, L. Doganay, F.Y. Enc, SIRT1 as a potential therapeutic target for treatment of nonalcoholic fatty liver disease, Med. Sci. Monit. 17 (5) (2011) HY5–HY9.

[10] D.G. Hardie, AMPK: a key regulator of energy balance in the single cell and the whole organism, Int. J. Obes. 32 (2008) S7–S12.

[11] C. Cantó, J. Auwerx, PGC-1α, SIRT1 and AMPK, an energy sensing network that controls energy expenditure, Curr. Opin. Lipidol. 20 (2009) 98–105.

[12] A. Purushotham, T.T. Schug, Q. Xu, S. Surapureddi, X. Guo, X. Li, Hepatocyte-specific deletion of SIRT1 alters fatty acid metabolism and results in hepatic steatosis and inflammation, Cell Metabol. 9 (2009) 327–338.

[13] T. Yamauchi, J. Kamon, H. Waki, K. Murakami, K. Motojima, K. Komeda, T. Ide, N. Kubota, Y. Terauchi, K. Tobe, H. Miki, A. Tsuchida, Y. Akanuma, R. Nagai, S. Kimura, T. Kadowaki, The mechanisms by which both heterozygous peroxisome proliferator-activated receptor gamma (PPARgamma) deficiency and PPARgamma agonist improve insulin resistance, J. Biol. Chem. 276 (44) (2001) 41245–41254.

[14] S. Francque, A. Verrijken, S. Caron, J. Prawitt, R. Paumelle, B. Derudas, P. Lefebvre, M.-R. Taskinen, I. Van Hul, I. Mertens, G. Hubens, E. Van Marck, P. Michielsen, L. Van Gaal, B. Staels, PPARα gene expression correlates with severity and histological treatment response in patients with non-alcoholic steatohepatitis, J. Hepatol. 63 (1) (2015) 164–173.

[15] W.N. Hannah, S.A. Harrison, Lifestyle and dietary interventions in the management of nonalcoholic fatty liver disease, Dig. Dis. Sci. 61 (2016) 1365–1374.

[16] M.R. Afrin, S. Arumugam, M.A. Rahman, V. Karuppagounder, R. Sreedhar, M. Harima, H. Suzuki, T. Nakamura, S. Miyashita, K. Suzuki, K. Ueno, K. Watanabe, Le Carbone, a charcoal supplement, modulates DSS-induced acute colitis in mice through activation of AMPKα and downregulation of STAT3 and caspase 3 dependent apoptotic pathways, Int. Immunopharm. 43 (2016) 70–78.

[17] J.C. Kerihuel, Effect of activated charcoal dressings on healing outcomes of chronic wounds, J. Wound Care 19 (2010) 208–215, 210–2, 214–5.

[18] H. Liang, P. Wang, X. Wang, N. Liu, X. Yue, D. Wang, J. Wang, X. Hao, Prospective randomized trial of prophylaxis of postoperative peritoneal carcinomatosis of advanced gastric cancer: intraperitoneal chemotherapy with mitomycin C bound to activated carbon particles, Zhonghua Wai Ke Za Zhi 41 (4) (2003) 274–277.

[19] H. Yamazaki, M. Fujieda, M. Togashi, T. Saito, G. Preti, J.R. Cashman, T. Kamataki, Effects of the dietary supplements, activated charcoal and copper chlorophyllin, on urinary excretion of trimethylamine in Japanese trimethylaminuria patients, Life Sci. 74 (2004) 2739–2747.

[20] P. Kuusisto, H. Vapaatalo, V. Manninen, J.K. Huttunen, P.J. Neuvonen, Effect of activated charcoal on hypercholesterolaemia, Lancet (London, England) 2 (8503) (1986) 366–367.

[21] R. Afrin, S. Arumugam, V. Soetikno, R.A. Thandavarayan, V. Pitchaimani, V. Karuppagounder, R. Sreedhar, M. Harima, H. Suzuki, S. Miyashita, M. Nomoto, K. Suzuki, K. Watanabe, Curcumin ameliorates streptozotocin-induced liver damage through modulation of endoplasmic reticulum stress-mediated apoptosis in diabetic rats, Free Radic. Res. 49 (2015) 279–289.

[22] M. Fujii, Y. Shibazaki, K. Wakamatsu, Y. Honda, Y. Kawauchi, K. Suzuki, S. Arumugam, K. Watanabe, T. Ichida, H. Asakura, H. Yoneyama, A murine model for non-alcoholic steatohepatitis showing evidence of association between diabetes and hepatocellular carcinoma, Med. Mol. Morphol. 46 (2013) 141–152.

[23] W. Liang, A.L. Menke, A. Driessen, G.H. Koek, J.H. Lindeman, R. Stoop, L.M. Havekes, R. Kleemann, A.M. van den Hoek, Establishment of a general NAFLD scoring system for rodent models and comparison to human liver pathology, PloS One 9 (12) (2014), e115922.

[24] R.D. Lillie, Further experiments with the masson trichrome modification of mallory's connective tissue stain, Biotech. Histochem. 15 (1) (1940) 17–22.

[25] R. Afrin, S. Arumugam, M.I.I. Wahed, V. Pitchaimani, V. Karuppagounder, R. Sreedhar, M. Harima, H. Suzuki, S. Miyashita, T. Nakamura, K. Suzuki, M. Nakamura, K. Ueno, K. Watanabe, Attenuation of endoplasmic reticulum stress-mediated liver damage by mulberry leaf diet in streptozotocin-induced diabetic rats, Am. J. Chin. Med. 44 (1) (2016) 87–101.

[26] M.S. Seo, J.H. Kim, H.J. Kim, K.C. Chang, S.W. Park, Honokiol activates the LKB1-AMPK signaling pathway and attenuates the lipid accumulation in hepatocytes, Toxicol. Appl. Pharmacol. 284 (2) (2015) 113–124.

[27] X.-N. Li, J. Song, L. Zhang, S.A. LeMaire, X. Hou, C. Zhang, J.S. Coselli, L. Chen, X.L. Wang, Y. Zhang, Y.H. Shen, Activation of the AMPK-FOXO3 pathway reduces fatty acid-induced increase in intracellular reactive oxygen species by upregulating thioredoxin, Diabetes 58 (2009) 2246–2257.

[28] J. Ertle, A. Dechêne, J.-P. Sowa, V. Penndorf, K. Herzer, G. Kaiser, J.F. Schlaak, G. Gerken, W.-K. Syn, A. Canbay, Non-alcoholic fatty liver disease progresses to hepatocellular carcinoma in the absence of apparent cirrhosis, Int. J. Canc. 128 (2011) 2436–2443.

[29] P.J. Neuvonen, P. Kuusisto, H. Vapaatalo, V. Manninen, Activated charcoal in the treatment of hypercholesterolaemia: dose-response relationships and comparison with cholestyramine, Eur. J. Clin. Pharmacol. 37 (3) (1989) 225–230.

[30] B.B. Zhang, G. Zhou, C. Li, AMPK: an emerging drug target for diabetes and the metabolic syndrome, Cell Metabol. 9 (2009) 407–416.

[31] D.B. Shackelford, R.J. Shaw, The LKB1-AMPK pathway: metabolism and growth control in tumour suppression, Nat. Rev. Canc. 9 (2009) 563–575.

[32] L. Zheng, W. Yang, F. Wu, C. Wang, L. Yu, L. Tang, B. Qiu, Y. Li, L. Guo, M. Wu, G. Feng, D. Zou, H. Wang, Prognostic significance of AMPK activation and therapeutic effects of metformin in hepatocellular carcinoma, Clin. Canc. Res. 19 (19) (2013) 5372–5380.

[33] Z. Xie, J. Zhang, J. Wu, B. Viollet, M.-H. Zou, Upregulation of mitochondrial uncoupling protein-2 by the AMP-activated protein kinase in endothelial cells attenuates oxidative stress in diabetes, Diabetes 57 (12) (2008) 3222–3230.

[34] K. Abdelmohsen, R. Pullmann, A. Lal, H.H. Kim, S. Galban, X. Yang, J.D. Blethrow, M. Walker, J. Shubert, D.A. Gillespie, H. Furneaux, M. Gorospe, Phosphorylation of HuR by Chk2 regulates SIRT1 expression, Mol. Cell. 25 (2007) 543–557.

[35] A. Salminen, J.M.T. Hyttinen, K. Kaarniranta, AMP-activated protein kinase inhibits NF-κB signaling and inflammation: impact on healthspan and lifespan, J. Mol. Med. (Berl.) 89 (2011) 667–676.

[36] J.T. Rodgers, C. Lerin, W. Haas, S.P. Gygi, B.M. Spiegelman, P. Puigserver, Nutrient control of glucose homeostasis through a complex of PGC-1α and SIRT1, Nature 434 (2005) 113–118.

[37] Y. Zhang, L.W. Castellani, C.J. Sinal, F.J. Gonzalez, P.A. Edwards, Peroxisome proliferator-activated receptor-gamma coactivator 1alpha (PGC-1alpha) regulates triglyceride metabolism by activation of the nuclear receptor FXR, Genes Dev. 18 (2004) 157–169.

[38] T.C. Leone, J.J. Lehman, B.N. Finck, P.J. Schaeffer, A.R. Wende, S. Boudina, M. Courtois, D.F. Wozniak, N. Sambandam, C. Bernal-Mizrachi, Z. Chen, J.O. Holloszy, D.M. Medeiros, R.E. Schmidt, J.E. Saffitz, E.D. Abel, C.F. Semenkovich, D.P. Kelly, PGC-1alpha deficiency causes multi-system energy metabolic derangements: muscle dysfunction, abnormal weight control and hepatic steatosis, PLoS Biol. 3 (4) (2005) e101.

[39] X. Qiang, L. Xu, M. Zhang, P. Zhang, Y. Wang, Y. Wang, Z. Zhao, H. Chen, X. Liu, Y. Zhang, Demethyleneberberine attenuates non-alcoholic fatty liver disease with activation of AMPK and inhibition of oxidative stress, Biochem. Biophys. Res. Commun. 472 (2016) 603–609.

[40] J.M. Ajmo, X. Liang, C.Q. Rogers, B. Pennock, M. You, Resveratrol alleviates alcoholic fatty liver in mice, Am. J. Physiol. Gastrointest. Liver Physiol. 295 (2008) G833–G842.

[41] R. Rahimian, E. Masih-Khan, M. Lo, C. van Breemen, B.M. McManus, G.P. Dubé, Hepatic over-expression of peroxisome proliferator activated receptor gamma2 in the ob/ob mouse model of non-insulin dependent diabetes mellitus, Mol. Cell. Biochem. 224 (2001) 29–37.

[42] N. Kubota, Y. Terauchi, H. Miki, H. Tamemoto, T. Yamauchi, K. Komeda, S. Satoh, R. Nakano, C. Ishii, T. Sugiyama, K. Eto, Y. Tsubamoto, A. Okuno, K. Murakami, H. Sekihara, G. Hasegawa, M. Naito, Y. Toyoshima, S. Tanaka, K. Shiota, T. Kitamura, T. Fujita, O. Ezaki, S. Aizawa, T. Kadowaki, PPAR gamma mediates high-fat diet-induced adipocyte hypertrophy and insulin resistance, Mol. Cell. 4 (4) (1999) 597–609.

[43] P.D. Miles, Y. Barak, W. He, R.M. Evans, J.M. Olefsky, Improved insulin-sensitivity in mice heterozygous for PPAR-gamma deficiency, J. Clin. Invest. 105 (3) (2000) 287–292.

[44] S.S.V.P. Sakamuri, R. Watts, A. Takawale, X. Wang, S. Hernandez-Anzaldo, W. Bahitham, C. Fernandez-Patron, R. Lehner, Z. Kassiri, Absence of Tissue Inhibitor of Metalloproteinase-4 (TIMP4) ameliorates high fat diet-induced obesity in mice due to defective lipid absorption, Sci. Rep. 7 (2017).

[45] H. Fujii, Y. Ikura, J. Arimoto, K. Sugioka, J.C. Iezzoni, S.H. Park, T. Naruko, H. Itabe, N. Kawada, S.H. Caldwell, M. Ueda, Expression of perilipin and adipophilin in nonalcoholic fatty liver disease; relevance to oxidative injury and hepatocyte ballooning, J. Atherosclerosis Thromb. 16 (6) (2009) 893–901.

[46] T. Tsujimoto, H. Kawaratani, T. Kitazawa, T. Hirai, H. Ohishi, M. Kitade, H. Yoshiji, M. Uemura, H. Fukui, Decreased phagocytic activity of Kupffer cells in a rat nonalcoholic steatohepatitis model, World J. Gastroenterol. 14 (39) (2008) 6036–6043.

[47] S. Zhong, L. Zhao, Y. Wang, C. Zhang, J. Liu, P. Wang, W. Zhou, P. Yang, Z. Varghese, J.F. Moorhead, Y. Chen, X.Z. Ruan, Cluster of differentiation 36 deficiency aggravates macrophage infiltration and hepatic inflammation by upregulating monocyte chemotactic protein-1 expression of hepatocytes through histone deacetylase 2-dependent pathway, Antioxidants Redox Signal. 27 (4) (2017) 201–214.

[48] V. Soetikno, F.R. Sari, A.P. Lakshmanan, S. Arumugam, M. Harima, K. Suzuki, H. Kawachi, K. Watanabe, Curcumin alleviates oxidative stress, inflammation, and renal fibrosis in remnant kidney through the Nrf2-keap1 pathway, Mol. Nutr. Food Res. 57 (9) (2013) 1649–1659.

[49] B. Li, L. Wang, Q. Lu, W. Da, Liver injury attenuation by curcumin in a rat NASH model: an Nrf2 activation-mediated effect? Ir. J. Med. Sci. 185 (2016) 93–100.

[50] L. Malaguarnera, R. Madeddu, E. Palio, N. Arena, M. Malaguarnera, Heme oxygenase-1 levels and oxidative stress-related parameters in non-alcoholic fatty liver disease patients, J. Hepatol. 42 (4) (2005) 585–591.

[51] C. Zou, C. Zou, W. Cheng, Q. Li, Z. Han, X. Wang, J. Jin, J. Zou, Z. Liu, Z. Zhou, W. Zhao, Z. Du, Heme oxygenase-1 retards hepatocellular carcinoma progression through the microRNA pathway, Oncol. Rep. 36 (5) (2016) 2715–2722.

[52] S.-M. Kim, J.P. Grenert, C. Patterson, M.A. Correia, CHIP(-/-)-Mouse liver: adiponectin-AMPK-FOXO-activation overrides CYP2E1-elicited JNK1-activation, delaying onset of NASH: therapeutic implications, Sci. Rep. 6 (2016) 29423.

[53] H. Nakagawa, A. Umemura, K. Taniguchi, J. Font-Burgada, D. Dhar, H. Ogata, Z. Zhong, M.A. Valasek, E. Seki, J. Hidalgo, K. Koike, R.J. Kaufman, M. Karin, ER stress cooperates with hypernutrition to trigger TNF-dependent spontaneous HCC development, Canc. Cell 26 (3) (2014) 331–343.

[54] M. Capurro, I.R. Wanless, M. Sherman, G. Deboer, W. Shi, E. Miyoshi, J. Filmus, Glypican-3: a novel serum and histochemical marker for hepatocellular carcinoma, Gastroenterology 125 (1) (2003) 89–97.

[55] T. Fujikawa, T. Shiraha, K. Yamamoto, Significance of des-gamma-carboxy prothrombin production in hepatocellular carcinoma, Acta Med. Okayama 63 (6) (2009) 299–304.